

Low-threshold induced side-scattering instability in the edge transport barrier at O-mode ECRH experiments in magnetic fusion devices

E.Z. Gusakov, A.Yu. Popov

Ioffe Institute, Saint-Petersburg, Russia

The possibility of electron plasma waves trapping in the steepest part of the tokamak's edge transport barrier leading to the excitation of low-threshold side-scattering absolute parametric decay instability in ordinary mode electron cyclotron resonance heating (ECRH) experiments is demonstrated. The instability is shown to be important for ECRH experiments in ITER.

Introduction. Three-wave interactions possible in nonlinear media for waves satisfying momentum and energy conservation principles (or decay conditions) give rise to so called parametric decay instabilities (PDIs) [1]. These instabilities, leading to the generation of daughter waves in the media, are excited in the presence of a strong pump wave if its amplitude exceeds a certain threshold determined by the daughter waves' energy losses [1]. In inhomogeneous media the PDI threshold is often determined by convective losses of daughter waves from the decay region [2,3]. In plasmas the PDIs cause anomalous absorption and reflection of electromagnetic pump waves if their thresholds are overcome, as in the case of ionosphere modification experiments [4] and laser fusion [5,6]. However, the theoretical analysis [7] predicted extremely high pump power-thresholds for any parametric decay instability that can accompany microwave propagation and damping in magnetic fusion devices in electron cyclotron resonance heating (ECRH) experiments. Therefore, until recently this method was thought to be free from anomalous phenomena and thus provide a predictable pump power deposition. It is widely used in current toroidal magnetic fusion devices and is planned for application in future fusion experiments. In particular, the fundamental harmonic ordinary mode (O1-mode) ECRH system is in preparation both for electron component heating and for controlling the neoclassical tearing mode in ITER. Such a system is also discussed for DEMO. However, over the last decade a number of anomalous phenomena – anomalous microwave backscattering [8,9], ion acceleration [10,11], an evident broadening of the ECRH power deposition profile [12,13] and radiation at sub-harmonics of the gyrotron frequency [14] – were discovered in ECRH experiments in different toroidal devices. The explanation of these observations turned out to be impossible within the framework of the traditional theoretical model [7]. Its extension, properly taking into account the presence of a non-monotonic (hollow) density profile often observed in experiments with ECRH [15,16], was proposed and then developed [17-20]. The key mechanism underlying the novel model is related to trapping of one of daughter waves (or even both of them) in the presence of a non-monotonic density profile. Such localization leads to the complete suppression of energy losses by the daughter wave from the decay layer and, consequently, to a drastic decrease (several orders of magnitude) in the decay instability power-threshold. The new model was used to analyze the most dangerous scenarios of low power-threshold parametric decays of both the second harmonic extraordinary microwave [19,20] and the fundamental harmonic ordinary microwave [21,22] in the vicinity of the local maximum of a non-monotonic density profile, leading to the excitation of localized upper hybrid waves. The possibility of substantial anomalous absorption has also been demonstrated [23].

However, the non-monotonic density profile does not appear to be the only cause of low power-threshold PDIs. In the present paper it is shown that quite unexpectedly the excitation of these phenomena can occur in the steepest region of the density profile, *i.e.* in the edge transport barrier, which usually exists in high performance discharges, and where, at first sight, the convective losses of daughter waves should be maximum and the conclusions of the theoretical analysis [7] should be justified. Nevertheless, it has been shown that the specific transparency domains afforded to intermediate frequency waves in regions with a high density gradient [24,25] result in their easy parametric excitation. As shown below, these waves can be trapped both in the direction of plasma inhomogeneity due to the edge transport barrier and along the magnetic field in its ripples associated with a finite number of toroidal magnetic field coils. Since the power thresholds of parametric decays leading to the excitation of localized daughter waves [17-22] turn out to be much lower than those predicted for the generation of non-localized daughter waves [7], absolute parametric decay instability (PDI) of megawatt microwave beams seems possible in future O1-mode ECRH experiments at ITER. This instability leads to the excitation of anomalously scattered ordinary waves and electron plasma waves (EPWs) trapped in the direction of plasma inhomogeneity and along the magnetic field.

2. Intermediate frequency wave trapping in strongly inhomogeneous plasmas. The usual approach to the analysis of intermediate frequency waves in inhomogeneous magnetized plasmas is the WKB approximation, which leads to the same conclusions on the wave transparency regions as the homogeneous plasma theory. However, strong plasma inhomogeneity at the plasma edge combined with a large value of the non-diagonal dielectric tensor component can lead to a significant change in the wave transparency [24,25], creating new transparency regions. The wavelength in this case remains much smaller than the plasma inhomogeneity scale length and therefore the effect can be accounted for in the WKB approximation modified by adding terms proportional to the derivatives of the dielectric tensor components [24]. To illustrate the manifestation of this phenomenon in the tokamak edge transport barrier (ETB), we introduce the local Cartesian coordinate system (x, y, z) . The coordinate x is related to the flux surface label, y - the coordinate perpendicular to the magnetic field line on the magnetic surface and z - the coordinate directed along the magnetic field line. The magnetic field in a narrow layer in the ETB has the form $B = \bar{B}(1 - \delta(x, y)\cos(Nz/R))$ with N being the number of toroidal coils, R - the major radius of tokamak and δ is the amplitude of magnetic ripples. The magnetic system of the ITER – the installation with a major radius $R = 6.2$ m – is designed with $N = 36$. The reduction of magnetic ripple from the value exceeding in the equatorial plane at the outboard plasma edge $\delta \approx 1\%$ down to $\delta \approx 0.3\%$ is discussed [26,27]. The amplitude of the electrostatic electron plasma (EP) wave $\phi(\mathbf{r}) = \psi(x, z)\exp(iq_y y + i\omega_L t) / 2 + c.c.$ is described by Poisson's equation $\hat{D}_{EPW}\psi = (\varepsilon(\omega_L)\Delta_{\perp} + \partial_x \varepsilon(\omega_L)\partial_x + \partial_x g(\omega_L)q_y + \eta(\omega_L)\partial_{zz})\psi = 0$ where ε , g , η are the components of the

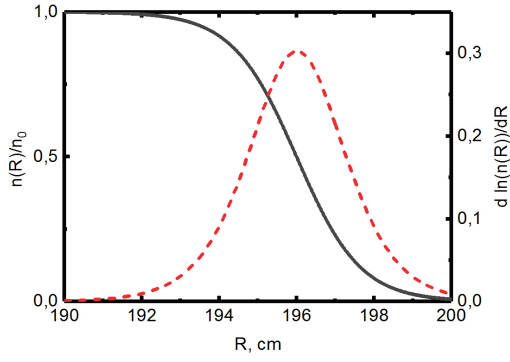


Figure 1. The density profile normalized to the density at the magnetic axis (solid line), and the profile of its derivation (dashed line).

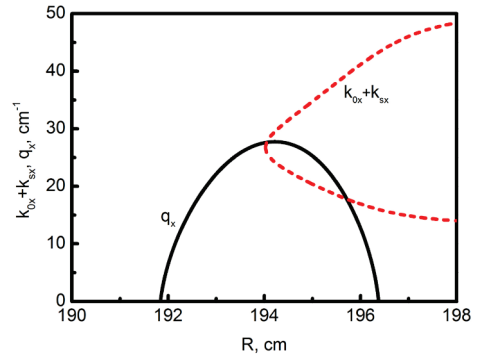


Figure 2. The dashed curve is the sum of the wave numbers of the pump and scattered ordinary waves. The solid curve is the wave number of the EPW;

$$f_0 = 170 \text{ GHz}, f_s = 168.86 \text{ GHz}, q_y^* = 30.45 \text{ cm}^{-1}.$$

cold-plasma dielectric tensor [28], $\Delta_{\perp} = \partial_{xx} - q_y^2$, $\partial_{\zeta} = \partial / \partial \zeta$, $\zeta = x, y$ and the term $\sim \partial_x \varepsilon(\omega_L)$ being much smaller than the term $\sim \partial_x g(\omega_L)$ by a factor of $\omega_L / \omega_{ce} \ll 1$ will be further neglected. The term

$Q = \partial_x g / \varepsilon|_{\omega_L}$ in the operator \hat{D}_{EPW} depends on the coordinates x and z . To illustrate the dependence on x ,

we take a density profile close to that expected in ITER in the edge transport barrier [26,27] (see figure 1).

The same figure shows its spatial derivative, which has a local maximum at x_m in the barrier region. Since

the function Q depends on the magnetic field, it has also a local minimum along the toroidal direction at

$z = 0$ between the two adjacent toroidal magnetic field coils where the pump power is launched. Then, we

approximate the function Q by quadratic dependencies over both coordinates

$Q \approx Q_0(1 - (x - x_m)^2 / (2l_x^2) + z^2 / (2l_z^2))$ around $x = x_m$, $z = 0$. Using this expansion yields

$$\hat{D}_{EPW} \psi \simeq \varepsilon(\omega_L, x_m) (\partial_{xx} + Q_0 q_y - q_y^2 - K_x^4 (x - x_m)^2) \psi - |\eta(\omega_L, x_m)| (\partial_{zz} - K_z^4 z^2) \psi = 0 \quad (1)$$

where $K_x = (Q_0 q_y / (2l_x^2))^{1/4}$ and $K_z = K_x (l_z^2 |\eta(\omega_L)| / l_x^2)^{-1/4}$. The solution to equation (1), representing the

EPW trapped both along the magnetic field and in the radial direction

$$\psi(\mathbf{r}) = \psi_{p,r} f_p(K_x(x - x_m)) f_r(K_z z), \psi_{p,r} = const, \quad (2)$$

is expressed in terms of the Hermite polynomials $f_p(Kx) = \sqrt{K / (\sqrt{\pi} 2^p p!)} \exp(-K^2 x^2 / 2) H_p(Kx)$.

Substituting (2) in (1) gives the quantization condition for its eigenfrequency

$$D_{EPW}(\omega_L^{p,r}) = \varepsilon(\omega_L^{p,r}) (Q_0 (\omega_L^{p,r}) q_y - q_y^2 - (2p + 1) K_x^2 (\omega_L^{p,r})) + (2r + 1) |\eta(\omega_L^{p,r})| K_z^2 (\omega_L^{p,r}) = 0. \quad (3)$$

These trapped EP waves, which propagate almost across the magnetic field, exist only in strongly inhomogeneous plasmas, where there are regions of transparency for those with a positive poloidal number.

If the density gradient is small or the parameter q_y^2 is too large, the plasma for such EPW turns out to be evanescent. It should be noted that the trapped EPW has another noteworthy property. According to (3) its

group velocity in the y direction determined as $v_{gy} = \partial D_{EPW} / \partial q_y / \partial D_{EPW} / \partial \omega_L^{p,r} \Big|_{\omega_L^{p,r}, q_y}$ takes the zero value at

$$q_y^* = Q_0 / 2.$$

3. Low-threshold parametric excitation of the EPW trapped in the ETB. We will show that the 2D localized EPWs can be easily excited in O1-mode ECRH experiments. Given the geometry of future experiments in ITER, we consider an ordinary pump wave propagating perpendicular to the magnetic field along the x - coordinate to the plasma core with its polarization vector being directed mostly along the magnetic field. In the framework of the WKB approximation it is represented as follows

$$\mathbf{E}_0 = \mathbf{e}_z \sqrt{2P_0 / (cw^2)} n_x(\omega_0, x)^{-1/2} \exp\left(- (y^2 + z^2) / (2w^2) + i \int_0^x k_x(\omega_0, x') dx' - i\omega_0 t\right) + c.c. \text{ where } P_0 - \text{ the}$$

pump power, w - the width of a beam, $c.c.$ - the term derived from the first one by complex conjugation,

$$n_{0x} = n_x(\omega_0) = ck_x(\omega_0) / \omega_0 = \sqrt{1 - \omega_{pe}^2 / \omega_0^2} - \text{ the wave refraction index, } \omega_{pe} - \text{ the Langmuir frequency. We}$$

analyse the pump wave decay in the ETB into the trapped EPW (2) and the side-scattered ordinary wave

$$\mathbf{E}_s(\mathbf{r}) = \mathbf{e}_z A_s(x) \exp(iq_y y + i\omega_s t) / 2 + c.c., \text{ whose amplitudes are described by the set of nonlinearly coupled}$$

equations

$$\begin{cases} \hat{D}_s A_s = \Delta_{\perp} A_s + \omega_s^2 / c^2 \eta(\omega_s) A_s = -i\kappa_{nl} \omega_s / c \Delta_{\perp} E_0^* \psi \\ \hat{D}_{EPW} \psi = i\kappa_{nl} c / \omega_s \Delta_{\perp} E_0 A_s \end{cases} \quad (4)$$

where $\kappa_{nl} = \omega_{pe}^2 / (\omega_0 \omega_{ce} \bar{B})$ - the nonlinear coupling coefficient [28], ω_{ce} - the electron cyclotron frequency.

The daughter O-mode wave has the reflection point determined through the equation $\eta(\omega_s, x_r) = n_{sy}^2$. For the

ITER parameters under consideration the reflection point x_r turns out to be in the EPW localization region.

To illustrate the case we plot in figure 2 the sum of wavenumbers of the pump and side scattered ordinary

waves $k_x(\omega_0) + k_x(\omega_s, q_y^*)$ shown by the dashed line and the EPW wavenumber $q_x = q_x(q_y^*)$ depicted by the

solid line. The waves parameters are $f_0 = 170$ GHz, $f_s = 168.86$ GHz, $q_y^* = 30.45$ cm⁻¹. In the close vicinity

of the points where the curves intersect the decay resonance condition, $\Delta K = k_x(\omega_0, x) + k_x(\omega_s, x) - q_x = 0$

is fulfilled and the parametric decay is possible. The Taylor series expansion of the potential

$\eta(\omega_s, x) \simeq n_{sy}^2 + (x_r - x) / L_r$ in the operator \hat{D}_s transforms the first line in (4) into the inhomogeneous Airy

equation. Its Green's function of this equation

$$G_s \{ \dots \} = \pi (c^2 L_r / \omega_s^2)^{1/3} \left(Bi(x - x_r) \int_{-\infty}^x dx' \dots Ai(x' - x_r) - Ai(x - x_r) \int_{-\infty}^x dx' \dots Bi(x' - x_r) \right) \text{ with } Ai, Bi \text{ being}$$

the Airy functions allows expressing the wave amplitude as a function of the nonlinear current

$A_s = -i\kappa_{nl} \omega_s / c G_s \{ \Delta_{\perp} E_0^* \psi \}$. Substituting A_s into the RHS of the second equation of system (4), we get the

equation for the EPW potential

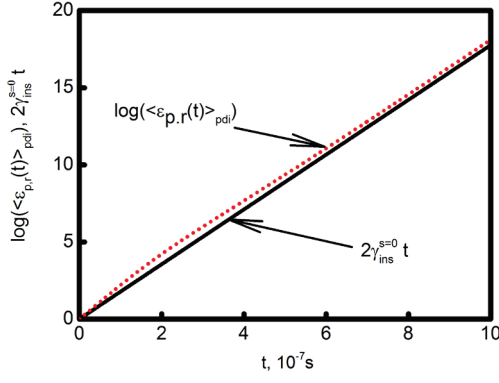


Figure 3. The amplification coefficients obtained numerically (dotted curve) and predicted analytically by (8) (solid curve) for the most unstable fundamental mode $s = 0$ and $P_0 = 1\text{MW}$.

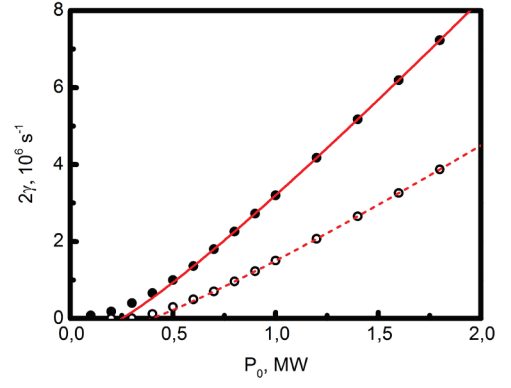


Figure 4. The growth rate on the pump power, $w = 2 \text{ cm}$. The solid ($\delta \approx 0.75\%$) and dashed ($\delta \approx 0.3\%$) curves are Eq. (8). The scattered circles (closed - $\delta \approx 0.75\%$, open - $\delta \approx 0.3\%$) are numerical solutions.

$$\hat{D}_{EPW}\psi = \kappa_{nl}^2 \Delta_{\perp} \left(E_0 G_s \left\{ \Delta_{\perp} (E_0^* \psi) \right\} \right) \quad (5)$$

To find a solution to (5), we utilize the procedure of perturbation theory [29]. In its first step, we neglect the nonlinear pumping described by the RHS of equation (5) and the daughter EPW energy losses along the y direction. A solution to the homogeneous version of equation (5) is determined through equation (2). In the second step of the perturbation procedure, we take into account the EPW energy loss along the coordinate y . For such a wave with the poloidal number $q_y^* = Q_0 / 2$ the group velocity tends to zero, and therefore the only mechanism of energy loss from the decay region in the y direction is diffraction, which is a slower process than convection. Therefore the EPWs, possessing the poloidal wavenumber close to this value are most unstable and excited first of all during the pump wave decay. The nonlinear interaction and energy loss make the amplitude $\psi_{p,r}$ no more constant, *i.e.* $\psi_{p,r} \rightarrow \psi_{p,r}(t, y)$ with $p = 28$, $r = 78$ at $\delta \approx 0.75\%$ and $p = 37$, $r = 83$ at $\delta \approx 0.3\%$. Substituting (2) into (5), multiplying both sides of the latter by $f_p(K_x x)^* f_r(K_z z)^*$ and integrating over x and z , we arrive at the equation describing the absolute PDI

$$\left(\partial / \partial t + i\Lambda_y \partial^2 / \partial y^2 \right) \psi_{p,r} = \gamma_0 \exp(-y^2 / w^2) \psi_{p,r} \quad (6)$$

where

$$\gamma_0 = i \frac{\omega_{pe}^4 (k_x^2(\omega_0) + q_y^{*2})^2}{\omega_0^2 \omega_{ce}^2 \left| \partial_{\omega_L} D_{EPW} \right|} \frac{2P_0}{cn_{0x} w^2 B^2} \left| \int_{x_m}^{\infty} dz |f_r(z)|^2 \exp\left(-\frac{z^2}{w^2}\right) \int_{-\infty}^{\infty} dx f_p(x)^* G_s \left\{ \exp\left(i \int_{x'}^x k_x(\omega_0) dx''\right) f_p(x') \right\} \right| -$$

the pumping rate, $\Lambda_y = \varepsilon(\omega_L, x_m) / \partial_{\omega_L} D_{EPW}$ - the diffraction coefficient and $\langle \dots \rangle$ - the averaging over the region of the EPW localization. Equation (6) describes the exponential growth of the EPW, which occurs when the pump power exceeds the threshold value P_0^{th} . If the pump power is significantly higher than the threshold value, $P_0 \gg P_0^{th}$, we can expand the function $\exp(-y^2 / w^2) \approx 1 - y^2 / w^2$ and get an analytical

approximation for the exponentially growing solution [20]

$$\psi_{p,r}(t, y) = \exp(\gamma_{ins}^s t + i\delta\omega_{ins}^s t) f_s(y / \delta_y), \quad \delta_y = \Lambda_y^{1/4} w^{1/2} / \sqrt[4]{\gamma_0} - \exp(-i\pi / 8 - i \arg(\gamma_0 / 4)) \quad (7)$$

$$\gamma_{ins}^s = \gamma_0' - (2s + 1) \sqrt{|\gamma_0| \Lambda_y / w^2} \sin(\arctan(\gamma_0'' / \gamma_0') / 2 + \pi / 4) \quad (8)$$

$$\delta\omega_{ins}^s = \gamma_0'' + (2s + 1) \sqrt{|\gamma_0| \Lambda_y / w^2} \cos(\arctan(\gamma_0'' / \gamma_0') / 2 + \pi / 4)$$

where $s \in \mathbb{Z}$. Though equation (8) is no more valid when the pump wave with the power $P_0 \geq P_0^{th}$ is marginally unstable, we can use it to estimate roughly the PDI power-threshold, which is determined by the EPW diffractive loss. To this end we set $\gamma_s = 0$ in equation (8), which gives the condition for P_0^{th}

$$\gamma_0'(P_0^{th}) = (2s + 1) \sqrt{|\gamma_0(P_0^{th})| \Lambda_y / w^2} \sin(\arctan(\gamma_0''(P_0^{th}) / \gamma_0'(P_0^{th})) / 2 + \pi / 4) \quad (9)$$

Then, we solve (6) numerically and plot the results in figure 3, where the temporal dependence of the wave energy in the region of the pump beam localization $\langle \varepsilon(t) \rangle_{pdi} = T_e / (\sqrt{\pi} w) \int_{-\infty}^{\infty} dy \exp(-y^2 / w^2) |\psi_{p,r}(t, y)|^2$ is shown in semi-logarithmic scale. The solid curve shows the same dependence but analytically predicted by (8). Being close to each other, they indicate a temporal growth of the EPW amplitude, which confirms the excitation of absolute PDI. A reasonable agreement between the numerical and analytical dependences is demonstrated. Figure 4 shows the dependence of the instability growth rate defined by equation (8) on the pump power at the pump beam width of 2 cm and magnetic field ripples $\delta \approx 0.3\%$ (dashed curve) and $\delta \approx 0.75\%$ (solid curve). The circles (open - $\delta \approx 0.3\%$ and closed - $\delta \approx 0.75\%$) are the numerical solutions to equation (6). The numerically calculated power thresholds is very low, $P_0^{th} = 287$ kW and $P_0^{th} = 113$ kW, correspondingly. Rough analytical estimates of the instability power thresholds in these cases provided by equation (9) overestimate their real values. It should be stressed that the obtained values of the absolute instability power threshold is three orders of magnitude smaller than the value predicted for the induced scattering instability by the standard theory [7], thus making this absolute PDI inevitable in ITER and leading to the risk of strong anomalous reflection of the ECRH power. At a pump power much higher than the power threshold of the instability excitation, analytical dependence (8) describes the growth rate with good accuracy. For the planned value of the ECRH power in a single beam of 1 MW planned for ITER the growth rate is equal to 3×10^6 s⁻¹. However, in the case when several heating beams cross the EPW localisation region, the growth rate will increase proportionally to the number of beams.

4. Conclusions. It is predicted that the electron plasma wave trapping in the edge transport barrier leads to the low power-threshold induced side-scattering absolute parametric decay instability of ordinary microwaves. At the magnetic field ripple $\delta \approx 0.75\%$, the minimum power-threshold of the PDI leading to scattering at the angle of 0.67π with frequency down-shift of 1.14 GHz is as small as 113 kW in a single microwave beam. At $\delta \approx 0.3\%$, the minimum power-threshold of the PDI leading to scattering at the angle of 0.65π with frequency down-shift of 1.13 GHz is 287 kW. The obtained values of the power-threshold

of absolute instability are three orders of magnitude smaller than the value predicted for the induced scattering instability by the standard theory [7]. This nonlinear effect, leading to anomalous reflection of heating power, could easily occur in O1-mode ECRH experiments at ITER, where multiple megawatt pump beams are planned for utilization. Undoubtedly, this effect can have a significant impact on the performance of the ECRH system at ITER and should be taken into account seriously when planning the future experiments.

Acknowledgements. *The PDI analytical treatment is supported under the Ioffe Institute state contract 0040-2019-0023, whereas the numerical modelling is supported under the Ioffe Institute state contract 0034-2021-0003*

- [1] D.J. Kaup, A. Reiman, A. Bers, *Reviews of Modern Physics* **51**, 275 (1979).
- [2] A.D. Piliya, *Proceedings of 10th Conf. Phenomena in Ionized Gases (Oxford)* 320, (1971).
- [3] M.N. Rosenbluth, *Phys. Rev. Lett.* **29**, 565 (1972).
- [4] T.B. Leyser, *Physics of Plasmas* **1**, 2003 (1994).
- [5] O.N. Krokhin, V.V. Pustovalov, A.A. Rupasov, V.P. Silin, G.V. Sklizkov, A.N. Starodub, V.T. Tikhonchuk, A.S. Shikanov, *Sov. Phys. - JETP Lett.* **22**, 21 (1975).
- [6] C.S. Liu, M.N. Rosenbluth, *Physics of Fluids* **19**, 967-971 (1976).
- [7] B.I. Cohen, R.H. Cohen, W.M. Nevins, T.D. Rognlien, *Rev. Mod. Phys.* **63**, 949 (1991).
- [8] E. Westerhof, S.K. Nielsen, J.W. Oosterbeek, M. Salewski, M.R. De Baar, W.A. Bongers, A. Bürger, B.A. Hennen, S.B. Korsholm, F. Leipold, D. Moseev, M. Stejner, and D. J. Thoen (the TEXTOR Team), *Phys. Rev. Lett.* **103**, 125001 (2009).
- [9] S.K. Nielsen, M. Salewski, E. Westerhof, W. Bongers, S.B. Korsholm, F. Leipold, J.W. Oosterbeek, D. Moseev, M. Stejner and the TEXTOR Team, *Plasma Phys. Control. Fusion* **55**, 115003 (2013).
- [10] S. Coda for the TCV Team, *Nucl. Fusion* **55**, 104004 (2015).
- [11] M. Martínez, B. Zurro, A. Baciero, D. Jiménez-Rey and V. Tribaldos, *Plasma Phys. Control. Fusion* **60**, 025024 (2018).
- [12] S. Eguilior, F. Castejron, E. de la Luna, A. Cappa, K. Likin, A. Fernández and TJ-II Team, *Plasma Phys. Control. Fusion* **45**, 105 (2003).
- [13] Yu.N. Dnestrovskij, A.V. Danilov, A.Yu. Dnestrovskij, S.E. Lysenko, A.V. Melnikov, A.R. Nemets, M.R. Nurgaliev, G.F. Subbotin, N.A. Solovev, D.Yu. Sychugov and S.V. Cherkasov, *Plasma Phys. Control. Fusion* **63**, 055012 (2021).
- [14] S.K. Hansen, S.K. Nielsen, J. Stober, J. Rasmussen, M. Stejner, M. Hoelzl, T. Jensen and the ASDEX Upgrade team, *Nucl. Fusion* **60**, 106008 (2020).
- [15] M.Yu. Kantor, A.J.H. Donne, R. Jaspers, H. van der Meiden and TEXTOR Team, *Plasma Phys. Control. Fusion* **51**, 055002 (2009).
- [16] A. Krämer-Flecken, X. Han, T. Windisch, J. Cosfeld, P. Drews, G. Fuchert, J. Geiger, O. Grulke, C. Killer, A. Knieps, Y. Liang, S. Liu, M. Rack and the W7-X team, *Plasma Phys. Control. Fusion* **61**, 054003 (2019).
- [17] E.Z. Gusakov, A.Yu. Popov, *Phys. Rev. Lett.* **105**, 115003 (2010).
- [18] E. Gusakov, A. Popov, *Europhys. Lett.* **99**, 15001 (2012).
- [19] A.Yu. Popov, E.Z. Gusakov, *Plasma Phys. Control. Fusion* **57**, 025022 (2015).
- [20] A.Yu. Popov, E.Z. Gusakov, *Europhys. Lett.* **116**, 45002 (2016).
- [21] E.Z. Gusakov, A.Yu. Popov, A.N. Saveliev, E.V. Sysoeva, *Plasma Phys. Control. Fusion* **59**, 075002 (2017).
- [22] E.Z. Gusakov, A.Yu. Popov, *Physics of Plasmas* **25**, 012101 (2018).
- [23] A.B. Altukhov, V.I. Arkhipenko, A.D. Gurchenko, E.Z. Gusakov, A.Yu. Popov, L.V. Simonchik, M.S. Usachonak, *Europhys. Lett.* **126**, 15002 (2019).

- [24] E.Z. Gusakov, M.A. Irzak, A.D. Piliya, JETP Lett. **65**, 25–31 (1997).
- [25] E.Z. Gusakov, V.V. Dyachenko, M.A. Irzak, O.N. Shcherbinin, S.A. Khitrov, Plasma Phys. Control. Fusion **52**, 075018 (2010).
- [26] K. Shinohara, T. Oikawa, H. Urano, N. Oyama, J. Lonroth, G. Saibene, V. Parail and Y. Kamada, Fusion Eng. Design **84**, 24 (2009).
- [27] N. Mitchell, A. Devred on behalf of the ITER Organisation, Domestic Agencies and Supplier Magnet Groups, Fusion Engineering and Design **123**, 17-25 (2017)
- [28] A.I. Akhiezer, I.A. Akhiezer, R.V. Polovin, A.G. Sitenko, K.N. Stepanov, Plasma Electrodynamics 1,2, Elsevier (1975).
- [29] E.Z. Gusakov, V.I. Fedorov, Sov. J. Plasma Phys. **5**, 263 (1979).